Available online at www.sciencedirect.com
SCIENCE DIRECT®
International Journal of Mass Spectrometry 244 (2005) 148–154
International Journal of Mass Spectrometry
www.elsevier.com/locate/ijms

A convenient method for calculation of ionic diffusion coefficients for accurate selected ion flow tube mass spectrometry, SIFT-MS

K. Dryahina [a,b], P. Španěl [a,*]

[a] *V. Čermák Laboratory, J. Heyrovský Institute of Physical Chemistry, Academy of Sciences of the Czech Republic, Dolejškova 3, 182 23, Prague 8, Czech Republic*
[b] *Charles University Prague, Faculty of Mathematics and Physics, Department of Electronics and Vacuum Physics, V Holešovičkách, Prague 8, Czech Republic*

Received 20 April 2005; received in revised form 7 June 2005; accepted 8 June 2005

Abstract

A method to calculate diffusion coefficients of ions important for the selected ion flow tube mass spectrometry, SIFT-MS, is presented. The ions, on which this method is demonstrated, include the SIFT-MS precursors $H_3O^+(H_2O)_{0,1,2,3}$, $NO\cdot^+(H_2O)_{0,1,2}$ and $O_2^{\bullet+}$ and the product ions relevant to analysis of breath trace metabolites ammonia ($NH_3^{\bullet+}(H_2O)_{0,1,2}$, $NH_4^+(H_2O)_{0,1,2}$), acetaldehyde ($C_2H_4OH^+(H_2O)_{0,1,2}$), acetone (CH_3CO^+, $(CH_3)_2CO^{\bullet+}$, $(CH_3)_2COH^+(H_2O)_{0,1}$, $(CH_3)_2CO\cdot NO^+$), ethanol ($C_2H_5OHH^+(H_2O)_{0,1,2}$) and isoprene ($C_5H_7^+$, $C_5H_8^{\bullet+}$, $C_5H_9^+$). Theoretical model of the (12, 4) potential for interaction between the ions and the helium atoms is used, with the repulsive part approximated by the mean hard-sphere cross section and the attractive part describing ion-induced dipole interactions. The reduced zero-field mobilities at 300 K are calculated using the Viehland and Mason theory [L.A. Viehland, S.L. Lin, E.A. Mason, At. Data Nucl. Data Tables, 60 (1995) 37–95], parameterised by a simple formula as a function of the mean hard-sphere cross section, and converted to diffusion coefficients using the Einstein relation. The method is tested on a set of experimental data for simple ions and cluster ions.

Keywords: Mobility; Diffusion; SIFT-MS; Ion geometry; Interaction potential

1. Introduction

Diffusion of ions through gases is a well-understood transport process closely related to the drift of ions through a gas in the presence of an electric field, which is characterized by the ionic mobility [1]. Recently, an accurate knowledge of diffusion coefficients for polyatomic and cluster ions has become important in the field of selected ion flow tube mass spectrometry, SIFT-MS [2,3]. Here, radial diffusion through inert helium carrier gas is the dominant loss process of ions in the analytical flow tube and the accuracy of the analysis [4] is directly influenced by the difference between the diffusion coefficients of the precursor (reagent) ions and the product ions characteristic of compounds present in trace amounts in the analysed air, liquid headspace or breath.

One of the most important applications of SIFT-MS is the trace gas analysis of exhaled breath that is currently attracting a great deal of attention because of its potential for the non-invasive study of metabolic processes and for clinical diagnosis and therapeutic monitoring [5]. Characteristic compounds are present in breath at concentrations typically near and below a part-per-million [2,3]. There is a considerable amount of data available on the mobilities of ions in various buffer gases [6–8], but these data do not include most of the ions of interest relating to SIFT-MS breath analysis [9]. The product ions involved in breath analysis range from small radical cations like NH_3^+ to large cluster ions like $C_2H_5OHH^+(H_2O)_2$ and their diffusion coefficients are generally different than those of the precursor ions. Therefore, differential diffusion occurs, which influences the magnitudes of the precursor and product ion signals. So it is important that the values of their diffusion coefficients are calculated consistently so that systematic errors are not amplified by the

* Corresponding author. Tel.: +420 2 6605 2112; fax: +420 2 8658 2307.
E-mail address: spanel@seznam.cz (P. Španěl).

1387-3806/$ – see front matter © 2005 Elsevier B.V. All rights reserved.
doi:10.1016/j.ijms.2005.06.001

subtraction of two similar values. Thus, there is a need for a straightforward and reliable method to calculate diffusion coefficients for characteristic SIFT-MS product ions in the helium carrier gas.

Diffusion coefficients of ions are related to their near-zero-field mobilities via the Einstein relation [1]. The actual value of the near-zero-field mobility for a given ion drifting through a buffer gas is entirely dependent on the form of the interaction potential between the ion and the atoms of the buffer gas. The problem of calculating the value of mobility from the interaction potential becomes mathematically accessible when the interaction potential can be treated as spherically symmetrical, in other words when the interaction energy of the ion and the buffer gas atom depends only on their distance and not on the angular configuration. The first rigorous ion mobility kinetic theory for such a case was developed by Viehland and Mason [10], providing a very good theoretical approximation based on the concept the momentum-transfer collision integral. For practical applications of this theory the values of these collision integrals were tabulated for the (n, 6, 4) model of ion–neutral atom interactions as functions of the effective ion temperature [10,11]. Thus, it is possible to build upon this reliable and often verified Viehland and Mason theory, as long as the actual interaction potential can be reasonably approximated by the spherically symmetrical model. This approach was first used for carbon cluster ions, C_x^+, for x up to 84, by von Helden et al. [12], by effectively approximating the interaction potential by a rectangular repulsive wall in the so-called hard-sphere model. The radius of the hard-sphere barrier was estimated by Monte-Carlo calculations of the average geometrical cross sections over numerous angular orientations of the cluster ions, in which the sizes of the individual atoms of the cluster ions were taken as their van der Waals radii [12].

This approach was further refined by de Gouw and coworkers [13,14] using the (12, 4) model potential, see Eq. (1) later, which is much more realistic than the rectangular wall for medium-sized organic ions and cluster ions. The parameters of this interaction potential were determined from the polarisabilty of the neutral N_2 molecules in the cluster ion describing the attractive induced-dipole interaction, and from the hard-sphere cross section determining the radius of the repulsive barrier for collisions with mean thermal kinetic energy. This theory was very successful in explaining the observed trends in experimentally determined mobilities of cluster ions (including the hydrated hydronium ions $H_3O^+(H_2O)_{1,2,3}$) drifting in helium and nitrogen buffer gases.

The main objective of the present study was to use the Viehland and Mason theory combined with the de Gouw et al. approach to estimate the parameters of the (12, 4) interaction potential to calculate the ion mobilities and diffusion coefficients of about 50 ions in helium, including several important for breath analysis using SIFT-MS, those few specific cluster ions for which experimental mobility values are available and for two negative ions that are of current interest in electron attachment research [15]. To test the validity of the method of calculation we also reproduce the mobility calculations for the ions included in the original paper by de Gouw et al. [13]. An early report on our work on diffusion calculations relevant to SIFT-MS was presented at a small international conference [16] and caused some interest amongst researchers using SIFT-MS and related flow tube techniques to quantitative trace gas analysis.

2. Method of calculation

The calculation is carried out in several steps: first the geometry of the molecular ion is determined, then the mean geometrical cross section for hard-sphere collisions is calculated, and finally mobility and diffusion coefficient are obtained from the approximate interaction potential parameterised using this hard-sphere cross section. Details of these calculation steps are given below.

2.1. Determination of ion geometries

We have used the *PC Spartan Pro* molecular modelling application (Wavefunction, Inc, Irvine, CA) to calculate the cluster ion geometries by the semi-empirical PM3 and the ab initio methods MP2/6-31G** and MP2/6-311+G**. The semi-empirical PM3 method was used to quickly calculate geometries of the precursor and product ions including the hydrates (calculations took 1–20 min on a 2.5 GHz Intel Celeron CPU). Ab initio methods using the Spartan program were used to validate the accuracy of the geometry calculations for H_3O^+ and its hydrates (using about 1–5 h CPU time). Cross section calculation using these ab initio geometries reproduced the cross sections calculated using the semi-empirical PM3 geometries to better than 0.7% accuracy. Thus, we decided to consistently use the Spartan PM3 semi-empirical method in order to obtain a uniform set of numerical data for all the ion geometries involved in this study. We have also used Gaussian 98 [17] to demonstrate that even when using more advanced B3LYP and MP3 levels of theory, the cross sections do not differ by more than 1% from our quick semi-empirical calculations. Thus, the choice of the actual theory behind the construction of the molecular model and calculation of the ion geometry is not critical with respect to the diffusion coefficients, and any molecular modelling application can be used, as long as the data are exportable to a set of Cartesian coordinates of the atoms. Note that our application [18] can open Spartan and Gaussian output files directly.

2.2. Calculation of the mean geometrical hard-sphere collision cross section

The hard-sphere cross section is determined numerically by projecting the molecular model onto a plane. The cross section is then calculated as the integrated area of the coordinates of the incoming carrier gas atoms perpendicularly to the

projection plane that interact with the atoms within the molecular ion. Each atom (identified by a subscript *i*) is represented in this projection by a circle with its van der Waals radius, r_i. Thus the range of coordinates around each nucleus in the ion where interactions is deemed to occur is the circle with a radius of $(r_i + r_{He})$, where r_{He} is the van der Waals radius of the He atom. The integration is performed numerically using an equi-spaced grid with 300×300 points. This integration is repeated for the ion oriented at 1000 different spherical angles, uniformly covering all orientations. We have also tried the Monte-Carlo approach used by Helden et al. [12], but we have found that the uniform grid provides more consistent and reliable results for a given number of operations. The van der Walls radii of the atoms within the ion are obtained from [19] as $r_H = 1.2$ Å, $r_C = 1.7$ Å, $r_N = 1.55$ Å, $r_O = 1.52$ Å, $r_B = 1.7$ Å, $r_F = 1.47$ Å, $r_{Cl} = 1.75$ Å. There is some uncertainty about the most appropriate value of the van der Walls radius of He atoms. We have chosen to use $r_{He} = 1.2$ Å [20], which provides optimum agreement between the calculated and experimental values for the mobilities/diffusion coefficients for the SIFT-MS precursor ions (H_3O^+, NO^+ and O_2^+). This r_{He} value is between the 1.0 Å adopted by de Gouw et al. [13] and another reported value of 1.4 Å [19].

2.3. Approximated interaction potentials and calculations of reduced zero field mobilities and diffusion coefficients

In this section we present the essential steps in the theory used in our work, but those readers only interested in practical calculations can use Eqs. (6) and (7) directly and skip the earlier part of this section.

The (12, 4) model of an ion–neutral molecule interaction represents the potential $V(r)$ as the sum of one repulsive term and one attractive term:

$$V(r) = \frac{B}{r^{12}} - \frac{C_4}{r^4}, \tag{1}$$

The coefficients B and C_4 have to be chosen to best characterise the real interactions. The attractive term C_4/r^4 describes the long-range charge/induced dipole interactions between the ions and the carrier gas atoms. Thus, the coefficient C_4 is given by the simple expression [11]:

$$C_4 = \frac{1}{2}\frac{q^2\alpha}{4\pi\varepsilon_0}, \tag{2}$$

q is the ionic charge, α is the polarisability of the neutral carrier gas atom, and $\varepsilon_0 = 8.854 \times 10^{-12}\ C^2\ J^{-1}\ m^{-1}$ is the permittivity of free space. The repulsive term B/r^{12} is an empirical representation of the short-range repulsive barrier (similar to that of the Lennard Jones potential [13]). The parameter B is chosen so that the radius of the repulsive barrier of the (12, 4) potential corresponds to the radius of the notional hard-sphere, $r_{hs} = \sqrt{\sigma_{hs}/\pi}$, representing the geometry of the molecular ion (see Fig. 1). The energy at which the repulsive barrier radius was considered is the mean thermal

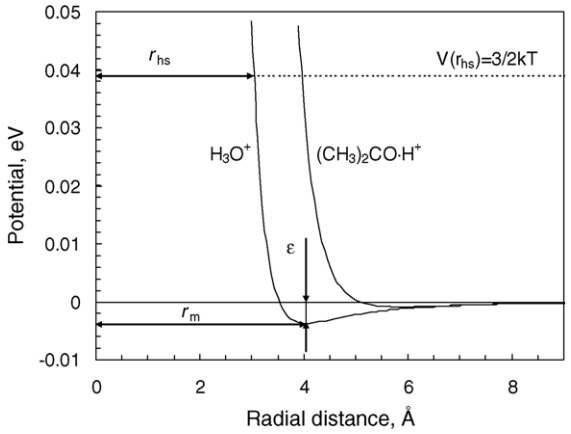

Fig. 1. The (12, 4) model interaction potentials for H_3O^+ and $(CH_3)_2COH^+$ ions and He atoms. The parameters of these potentials are determined from the polarisability of the He atom and from the hard-sphere radii, r_{hs}, for collision of these ions with a helium atom calculated from their geometry and the van der Waals radii of the individual atoms in the ions. ε and r_m are the depth and position, respectively, of the minima of these potentials that are used to obtain the collision integrals.

energy of the collisions [13]. Thus, a boundary condition on the potential (1) is:

$$V(r_{hs}) = \frac{3}{2}kT, \tag{3}$$

k is Boltzmann's constant and T is the temperature. The parameter B can be expressed analytically by solving Eqs. (1) and (3) as:

$$B = \left(\frac{\sigma_{hs}}{\pi}\right)^4 \left(C_4 + \frac{3}{2}kT\left(\frac{\sigma_{hs}}{\pi}\right)^2\right). \tag{4}$$

Thus, the form of the (12, 4) model potential is now entirely defined by just two parameters: the polarisability of the neutral atom, α, and the effective hard-sphere cross section for the ion-atom system, σ_{hs}.

According to the Viehland and Mason mobility theory [11], the collision integral $\overline{\Omega}^{(1.1)}$ is determined from the depth, ε, and the position, r_m, of the minimum in the interaction potential, V (see Fig. 1), as:

$$\overline{\Omega}^{(1.1)}(T, \varepsilon, r_m) = \Omega^{(1.1)^*}(T^*) \times \pi r_m^2, \tag{5}$$

Here, $\Omega^{(1.1)^*}$ is the dimensionless value obtained by interpolating between the tabulated values from [11], which are given as a function of the dimensionless relative temperature $T^* = kT/\varepsilon$. All the information about the ion-neutral potential is now for a given T contained in the momentum-transfer collision integral, $\overline{\Omega}^{(1.1)}$. Thus, it is clear that for the diffusion of ions at a temperature of 300 K in He ($\alpha = 0.205\ cm^{-2}$) [21] the only variable influencing the value of the collision integral obtained by following Eqs. (1)–(5) is the hard-sphere cross section, σ_{hs}. It is facile to approximate the variation of $\overline{\Omega}^{(1.1)}$

(in the units of Å^2) by a simple parameterised function:

$$\overline{\Omega}^{(1.1)} = 0.975 \quad \sigma_{hs} + \left(\frac{40.65}{\sigma_{hs}}\right)^2 \tag{6}$$

This simple approximation allows quick calculations of the collision integrals in the range of σ_{hs} (in the units Å^2) from 20 to 110 to an accuracy better than 1% without having to repeat the detailed calculations for every ion type. Finally, it is a straightforward matter to use the original Viehland and Mason equation [11] to calculate the reduced near-zero-field mobility:

$$K = \frac{3q}{16N}\left(\frac{2\pi}{kT}\right)^{1/2}\left(\frac{m+M}{mM}\right)^{1/2}\frac{1}{\overline{\Omega}^{(1.1)}(T)}, \tag{7}$$

Here, q is the ion charge, N is the number density of the neutral gas atoms (taken as the Loschmidt number, N_0, for the calculation of the reduced mobility, K_0, at atmospheric pressure, p_0), m is the ion mass, M is the mass of the neutral atoms, and k is the Boltzmann constant. The diffusion coefficient, D, is obtained from K using the Einstein relation combined with the conversion from atmospheric pressure to the nominal pressure of p_1 = 1 Torr = 133 Pa, which is typical of that used for the helium carrier gas in SIFT-MS. Thus,

$$D = K_0\frac{kT}{q}\frac{p_0}{p_1}, \tag{8}$$

To facilitate comparison with published diffusion coefficients the values are presented in this paper in the traditional units of cm^2 s^{-1}.

Additionally, as suggested by a reviewer of this paper, the calculation can be further refined by including the additional attraction term C_6 in the interaction potential describing London dispersion forces accounting for the polarizability of the ion [22–24]. It is known that this interaction can have a significant effect on the rate constants of ion–molecule reactions [25]. When this sixth order contribution is included, the values of $\overline{\Omega}^{(1.1)}$ reduce on average by 1.3% and the numerical parameters in Eq. (6) become 0.962 and 40.38 A^2.

3. Results

3.1. Calculations for a set of selected molecular and cluster ions

The compiled results of calculations are summarised in Table 1. The list of ions is given in the second column, grouped into several classes: the SIFT-MS precursor ions used for trace gas analysis are $H_3O^+(H_2O)_{0,1,2,3}$, $NO^+(H_2O)_{0,1,2}$ and $O_2^{\bullet+}$. Some SIFT-MS product ions are grouped in association with the compound, M, from which they originate in the ion–molecule reactions exploited for SIFT-MS analysis; they are variously protonated products, MH^+, formed in the reactions of M with H_3O^+, the hydrates of MH^+, the parent cations M^+ produced in the NO^+ or $O_2^{\bullet+}$ reactions, fragment ions formed by the dissociation of the parent cations, M^+, and an NO^+ adduct with CH_3CN. Some other ions that are not directly involved in SIFT-MS breath analysis, but which are either for validation and comparison with previously published data, are also included. Finally, the two negative ions included are some ions relevant to recent studies of electron attachment branching ratios [15].

Ion geometries were calculated for all of these ions, and presented in the form of Cartesian x, y, z coordinates and represented graphically as three-dimensional molecular models to allow visual inspection of their structures. For the sake of brevity, we do not list the detailed geometries in this paper, but we have included the x, y, z Cartesian coordinates in the on-line supporting material (see Appendix A). The values of hard-sphere cross sections are calculated, in Å^2, specifically for the collisions of the ions with He atoms (see Section 2.2). They are rounded to one decimal place and their numerical accuracy is better than ±2%. However, this has to be qualified by a reminder that the very concept of using van der Waals radii to represent the repulsive interaction between ions and atoms is in itself just an approximation. The calculated values of the reduced mobilities of ions in He using the (12, 4) model potential are given in the traditional units of cm^2 V^{-1} s^{-1} at atmospheric pressure; their numerical accuracy is ±3%. The results of calculation additionally including the C_6 term of the interaction potential (12, 6, 4) are given for several ions, where the ion polarisability could be estimated. The values of diffusion coefficients in He are calculated for a pressure of 1 Torr and for a temperature of 300 K.

4. Discussion

The most obvious feature of these collected results is they demonstrate that for ions relevant to SIFT-MS it is the geometrical size of the ion that is the dominant factor that determines the value of the mobility and diffusion coefficients in helium. To illustrate this, the variation of the reduced mobility, K_0, with the hard-sphere cross section, σ_{hs}, is presented in Fig. 2. It can be seen that the variation is dominated by σ_{hs}, the

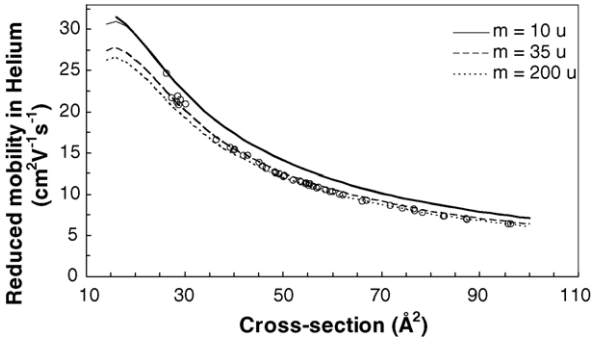

Fig. 2. Variation of the reduced mobility of ions from Table 1 with the hard-sphere cross section, σ_{hs}, for their collisions with He atoms. The thin lines are results of exact calculations using Eq. (5), the thick line uses approximation by Eq. (6), the data points are the individual values calculated for the actual ionic masses, m Eq. (7) for the three values of m given.

Table 1
Hard-sphere cross sections, reduced mobilities and diffusion coefficients

Ion type	Ion	Mass (u)	σ_{hs} (Å^2)	Polarizability (10^{-24} cm^3)	K_o (cm^2 V^{-1} s^{-1})			Diff. coeff. D (cm^2 s^{-1})
					(12, 4)	(12, 6, 4)	Experimental	
SIFT-MS precursor ions								
	H_3O^+	19	29.1		21.4		21.5 ± 1.5[a]	421
	$H_3O^+(H_2O)$	37	39.3		15.6		17.2 ± 1.2[a]	307
	$H_3O^+(H_2O)_2$	55	50.4		12.2		13.9 ± 1.0[a]	239
	$H_3O^+(H_2O)_3$	73	60.0		10.3		11.5 ± 0.8[b]	202
	NO^+	30	28.4	1.7	21.1	21.4	21.3 ± 1.5[c]	416
	$NO\cdot^+H_2O$	48	36.4		16.6		16.6 ± 1.2[a]	326
	$NO\cdot^+(H_2O)_2$	66	48.5		12.5			246
	$O_2^{\bullet+}$	32	28.9	1.6	20.8	21.0	21.8 ± 1.5[c]	409
SIFT-MS product ions								
Ammonia	$NH_3^{\bullet+}$	17	28.6	2.3	21.9	22.2	23.0 ± 1.6[c]	430
	$NH_3^{\bullet+}H_2O$	35	40.2		15.4			302
	$NH_3^{\bullet+}(H_2O)_2$	53	54.8		11.3			223
	NH_4^+	18	30.3		20.9		21.9 ± 1.5[c]	411
	$NH_4^+H_2O$	36	42.8		14.6			287
	$NH_4^+\cdot(H_2O)_2$	54	55.4		11.2			220
Acetaldehyde	$C_2H_4OH^+$	45	42.0	4.3	14.7	14.9		289
	$C_2H_4OH^+(H_2O)$	63	46.6		13.1			257
	$C_2H_4OH^+(H_2O)_2$	81	57.0		10.8			212
Acetone	CH_3CO^+	43	40.0		15.3			301
	$(CH_3)_2CO^{\bullet+}$	58	48.4	6.3	12.6	12.9		248
	$(CH_3)_2COH^+$	59	49.3		12.4			243
	$(CH_3)_2COH^+(H_2O)$	77	59.5		10.3			203
	$(CH_3)_2CO\cdot NO^+$	88	55.3		11.1			218
Ethanol	$C_2H_5OHH^+$	47	45.8	5.11	13.4	13.7		264
	$C_2H_5OHH^+(H_2O)$	65	53.5		11.5			226
	$C_2H_5OHH^+(H_2O)_2$	83	62.2		9.9			195
Isoprene	$C_5H_7^+$	67	57.2		10.8			212
	$C_5H_8^{\bullet+}$	68	53.6	9.99	11.5	11.6		226
	$C_5H_9^+$	69	56.2		11.0			215
Monoterpenes	Limonene	136	82.8		7.3			144
$C_{10}H_{16}^{\bullet+}$	Camphene	136	75.2		8.1			159
	Myrcene	136	83.9		7.2			142
	2-Carene	136	82.3		7.4			145
Nicotine	$C_{10}H_{14}N_2^{\bullet+}$	162	82.6		7.3			144
Other ions								
Boron	B^+	10.8	26.4	3.03	24.6	24.8	25.0 ± 1.1[e]	484
Aromatic hydrocarbons	$C_6H_6^{\bullet+}$	78	58.7	10.32	10.5	10.6	11.8 ± 0.3[b]	206
	$C_6H_6H^+$	79	54.5		11.3		11.6 ± 0.4[b]	222
	$C_7H_8H^+$	93	61.5		10.0		12.3 ± 2.0[d]	196
	$C_8H_{10}H^+$	107	71.8		8.6		11.1 ± 2.0[d]	168
	$C_6H_5^+$	77	52.2		11.7		11.7 ± 0.4[b]	230
	$C_{12}H_{10}^{\bullet+}$	154	78.5		7.8		7.6 ± 0.3[b]	153
	$C_{10}H_8^{\bullet+}$	128	74.2	16.5	8.3	8.4	8.8 ± 0.3[b]	162
	$C_{12}H_{12}^{\bullet+}$	156	87.4		6.9		7.6 ± 0.3[b]	136
Ketone dimmers	$(CH_3COCH_3)_2H^+$	117	76.6		8.1		10.6 ± 2.0[d]	160
	$(CH_3COC_2H_5)_2H^+$	145	87.2		7.0		7.2 ± 2.0[d]	137
	$(C_2H_5COC_2H_5)_2H^+$	173	95.8		6.4		5.7 ± 2.0[d]	125
	$(CH_3COCH_3)_2\cdot NO^+$	146	86.64		7.4		7.5 ± 0.4	145
	$(CH_3COCH_3)_3\cdot NO^+$	204	107.37		6.3		7.3 ± 0.5	124
Ammonia clusters	$NH_4^+(NH_3)$	35	45.2		13.8		16.6 ± 0.4[b]	271
	$NH_4^+(NH_3)_2$	52	55.2		11.3		12.2 ± 0.4[b]	221
	$NH_4^+(NH_3)_3$	69	67.1		9.2		12.1 ± 0.4[b]	182

Table 1 (*Continued*)

Ion type	Ion	Mass (u)	σ_{hs} (Å^2)	Polarizability (10^{-24} cm^3)	K_o (cm^2 V^{-1} s^{-1})			Diff. coeff. D (cm^2 s^{-1})
					(12, 4)	(12, 6, 4)	Experimental	
NO^+, acetonitrile	NO^+CH_3CN	71	50.1		12.1		12.3 ± 0.3[b]	239
	$NO^+(CH_3CN)_2$	112	76.8		8.0		8.2 ± 0.2[b]	157
	$NO^+(CH_3CN)_3$	153	96.3		6.4		7.5 ± 0.5[b]	125
Negative ions	Cl^-	35.4	27.3	2.18	21.6	21.8	20.3 ± 1.4[a]	426
	$C_6F_5Cl^{\bullet -}$	202	66.2		9.2			180

[a] Taken from [7].
[b] Taken from [13].
[c] Taken from [6].
[d] Taken from [4].
[e] Taken from [26].

variation with the mass of the ion being relatively small. This is because the reduced mass, μ, for ions interacting with He atoms does not vary significantly with the ion mass (μ only varying from 3.3 to 3.9 for ions ranging from H_3O^+ (19 u) to $C_{10}H_{14}N_2^+$ (160 u). The set of three lines in Fig. 2 represents the separate contributions of the reduced mass and the collision integral to the K_0 value derived using Eq. (7).

It is interesting to investigate the differences in the results of the calculations between the isomeric forms of monoterpenes. We have included four different isomers of $C_{10}H_{16}^{\bullet +}$ (limonene, camphene, myrcene and 2-carene). Results for the three planar isomers that are open chain (myrcene) or have only a single six member cycle (limonene and 2-carene) are similar (ranging from 7.2 to 7.4 cm^2 V^{-1} s^{-1}) but the result for the more compact molecule of camphene shows smaller hard sphere cross section and thus about 10% higher mobility (8.1 cm^2 V^{-1} s^{-1}).

Note again that in the present work we have used r_{He} = 1.2 Å and in the calculation of the hard-sphere cross section we have considered the individual interactions between the He atom and the composite atoms of the molecular ions. Also, we have found that the ion-induced dipole interaction must be included in the model in order to cover the ions ranging from relatively small species like B^+ and NO^+ to large cluster ions. An extreme assumption of the rectangular hard-sphere only interaction (equating $\sigma_{hs} = \bar{\Omega}^{(1.1)}$) would lead for these small ions to mobilities about 6% higher then the more accurate (12, 4) approximation using the Eq. (6). Further refinement of the interaction potential by including the effects of the polarizability of the ion and the dispersion interaction (12, 6, 4) only increases the calculated mobilities and diffusion coefficients by 1.3% on average. For practical purposes, the choice of the interaction potential is thus reflected to the choice of numerical parameters of Eq. (6) used in the calculation.

It is now a straightforward procedure to calculate the diffusion coefficients for specific product ions formed in SIFT-MS analyses and thus to account more accurately for differential diffusion of precursor and product ions, thus minimizing errors due to this phenomenon. Indeed, this can now be achieved with confidence by parameterizing the diffusion coefficients as part of the analytical procedure.

4.1. Comparison with experimental values

The experimental values for K_0 in Table 1 are taken from [4,6,7,13,26] and are given with the error bars as reported in the original publications. Our calculated values for the SIFT-MS precursor ions agree very well with the established values, the result for H_3O^+ being only 0.5% below the experimental value, for NO^+ it is 1% below the experimental value and for O_2^+ it is greater being 5% below the experimental value. Since the stated uncertainty for these three experimental values is ±7% we can say that the present calculations are in good agreement with these experimental values. The situation for the hydrated hydronium ions is somewhat less satisfactory, the deviation from the experimental values ranging from 9 to 12%. It is worthy of note that de Gouw et al. [13] used smaller value of r_{He} to rationalize the calculation for these ions.

There are only two previous experimental results for K_0 for the ions in the group of SIFT-MS product ions, which are for the NH_3^+ and NH_4^+ ions. The present calculated values agree well with these within the quoted experimental error (see Table 1). In the group of other ions chosen because of the availability of experimental data, it can be seen that there is good agreement between our calculated values and the experimental values. The discrepancies vary from −24 to +12% of the experimental value with a mean difference of −8%. For the Cl^- negative ions the agreement between theory and experiment is within the reported experimental error bar. There is no experimental value of K_0 for $C_6F_5Cl^-$; the present calculated value can be used to assess the experimental results on the product ion branching ratio in electron attachment to C_6F_5Cl [15].

Use of the (12, 6, 4) model potential in every case gave better agreement with the experimental values than the simpler (12, 6) model, albeit the change was only in the range from 0.8 to 2%.

5. Concluding remarks

The present method of calculation of reduced mobilities allows the diffusion coefficients of ions important for SIFT-

MS analysis and for similar quantitative flow tube analytical methods (in which diffusive loss of ions is a factor in the gas analysis) to be calculated easily and quickly. Using a combination of a semi-empirical molecular modelling to determine the ionic geometry and the software implementing the method described in this article [18], the value of the diffusion coefficient for ions of arbitrary size and complexity can be obtained within a fraction of an hour to an accuracy of better than ±20%. In particular, we expect that researches in the various fields of flow tube mass spectrometry will find this a useful approach to the assessment of the influence that differential diffusion may have on their analyses. Thus, we have not only presented the data resulting from our calculations, but also described the numerical method of calculation in a concise way, so that other scientists utilizing SIFT-MS for trace gas analysis can exploit it to readily calculate diffusion coefficients for ions of interest without having to study the details of the underlying theories. As a further help to complement this paper we are releasing a user friendly supporting software application for the calculations of diffusion coefficients [18].

Acknowledgements

We would like to thank David Smith for providing the stimulation for this work, for useful discussions and for reading and correcting the manuscript. This work was in part supported by the Grant Agency of Czech republic Grant Agency of the Czech Republic (project number 202/03/0827) and by the Academy of Sciences of the Czech Republic (project number K4040110).

Appendix A. Supplementary data

Supplementary data associated with this article can be found, in the online version, at doi:10.1016/j.ijms.2005.06.001.

References

[1] E.W. McDaniel, E.A. Mason, The Mobility and Diffusion of Ions in Gases, John Wiley, New York, 1973, Chap. 6.
[2] P. Španěl, D. Smith, Med. Biol. Eng. Comput. 34 (1996) 409.
[3] D. Smith, P. Španěl, in: J. Lindon, G. Trantner, J. Holmes (Eds.), Encyclopedia of Spectroscopy and Spectrometry, Mass Spectrometry, Academic Press, London, 1999, p. 2092.
[4] P. Španěl, D. Smith, J. Am. Soc. Mass. Spectrom. 12 (2001) 863.
[5] A. Amman, D. Smith (Eds.), Breath Analysis for Clinical Diagnosis and Therapeutic Monitoring, World Scientific, Singapore, 2005.
[6] H.W. Ellis, R.Y. Pai, E.W. McDaniel, E.A. Mason, L.A. Viehland, At. Data Nucl. Data Tables 17 (1976) 177.
[7] H.W. Ellis, E.W. McDaniel, D.L. Albritton, L.A. Viehland, S.L. Lin, E.A. Mason, At. Data Nucl. Data Tables 22 (1978) 179.
[8] L.A. Viehland, S.L. Lin, E.A. Mason, At. Data Nucl. Data Tables 60 (1995) 37.
[9] A.M. Diskin, P. Španěl, D. Smith, Physiol. Meas. 24 (2003) 107.
[10] L.A. Viehland, E.A. Mason, Ann. Phys. 91 (1975) 499.
[11] L.A. Viehland, E.A. Mason, W.F. Morrison, M.R. Flannery, At. Data Nucl. Data Tables 16 (1975) 495.
[12] G. von Helden, M.T. Hsu, N. Gotts, M.T. Bowers, J. Phys. Chem. 97 (1993) 8182.
[13] J.A. de Gouw, M. Krishnamurthy, V.M. Bierbaum, S.R. Leone, Int. J. Mass Spectrom. Ion Proc. 167–168 (1997) 281–289.
[14] J.A. de Gouw, L.N. Ding, M. Krishnamurthy, H.S. Lee, E.B. Anthony, V.M. Bierbaum, S.R. Leone, J. Chem. Phys. 105 (23) (1996) 10398.
[15] T.M. Miller, A.A. Viggiano, Phys. Rev. A 70 (2004) 1–11.
[16] K. Dryahina, P. Španěl, in: J. Safrankova (Ed.), WDS'04 Proceedings of Contributed Papers, Part II, MATFYZPRESS, Prague, 2004, p. 407.
[17] M.J. Frisch, G.W. Trucks, H.B. Schlegel, G.E. Scuseria, M.A. Robb, J.R. Cheeseman, V.G. Zakrzewski, J.A. Montgomery Jr., R.E. Stratmann, J.C. Burant, S. Dapprich, J.M. Millam, A.D. Daniels, K.N. Kudin, M.C. Strain, O. Farkas, J. Tomasi, V. Barone, M. Cossi, R. Cammi, B. Mennucci, C. Pomelli, C. Adamo, S. Clifford, J. Ochterski, G.A. Petersson, P.Y. Ayala, Q. Cui, K. Morokuma, D.K. Malick, A.D. Rabuck, K. Raghavachari, J.B. Foresman, J. Cioslowski, J.V. Ortiz, B.B. Stefanov, G. Liu, A. Liashenko, P. Piskorz, I. Komaromi, R. Gomperts, R.L. Martin, D.J. Fox, T. Keith, M.A. Al-Laham, C.Y. Peng, A. Nanayakkara, C. Gonzalez, M. Challacombe, P.M.W. Gill, B. Johnson, W. Chen, M.W. Wong, J.L. Andres, C. Gonzalez, M. Head-Gordon, E.S. Replogle, J.A. Pople, Gaussian 98, Revision A. 6, Gaussian Inc., Pittsburgh PA, 1998.
[18] K. Dryahina, DiffusionCalc software, 2005. Available on-line at http://www.jh-inst.cas.cz/~dryahina/.
[19] A. Bondi, J. Phys. Chem. 68 (3) (1964) 441.
[20] A.M. James, M.P. Lord, Macmillan's Chemical and Physical Data, Macmillan, London, 1992.
[21] T.M. Miller, B. Bederson, Adv. At. Mol. Phys. 13 (1977) 1.
[22] K. Dryahina, in: J. Safrankova (Ed.), WDS'03 Proceedings of Contributed Papers, Part II, MATFYZPRESS, Prague, 2003, p. 481.
[23] S. Selle, U. Riedel, Transport Coefficients of Reacting Air at High Temperatures, AIAA Paper 2000-0211, American Institute of Aeronautics and Astronautics, Reno, 2000.
[24] A.D. Koutselos, E.A. Mason, J. Chem. Phys. 85 (4) (1986) 2154.
[25] B. Eichelberger, T.P. Snow, V.M. Bierbaum, J. Am. Soc. Mass Spectrom. 14 (2003) 501.
[26] R.W. Simpson, P.W. Harland, R.G.A.R. Maclagan, D. Smith, N.G. Adams, Int. J. Mass Spectrom Ion Proc. 90 (1989) 193.